

## Modeling soil erosion on steep sagebrush rangeland before and after prescribed fire

Corey A. Moffet<sup>a</sup>, Frederick B. Pierson<sup>b,\*</sup>, Peter R. Robichaud<sup>c</sup>,  
Kenneth E. Spaeth<sup>d</sup>, Stuart P. Hardegee<sup>b</sup>

<sup>a</sup> USDA–Agricultural Research Service, U.S. Sheep Experiment Station, Dubois, Idaho 83423 (formerly Northwest Watershed Research Center, Boise, Idaho 83712), United States

<sup>b</sup> USDA–Agricultural Research Service, Northwest Watershed Research Center, Boise, Idaho 83712, United States

<sup>c</sup> USDA–Forest Service, Rocky Mountain Research Station, Moscow, Idaho 83843, United States

<sup>d</sup> USDA–Natural Resources Conservation Service, Central National Technology Support Center, Fort Worth, Texas 76115, United States

### Abstract

Fire in sagebrush rangelands significantly alters canopy cover, ground cover, and soil properties which influence runoff and erosion processes. Runoff can be generated more quickly and in larger volume following fire resulting in increased risk of severe erosion and downstream flooding. The Water Erosion Prediction Project (WEPP) model was developed to predict erosion on cropland, forest, and rangeland. WEPP is a tool that has potential to model the effect of fire on hillslope hydrological processes and help managers address erosion and runoff risks following fire. Experimental results on a steep (35 to 50% slope) sagebrush site suggest that rill erosion is the dominant erosion process following fire and the WEPP parameterization equations related to the rill erosion process need improvements. Rill detachment estimates could be improved by modifying regression-estimated values of rill erodibility. Also, the interactions of rill width and surface roughness on soil shear stress estimates may also need to be modified. In this paper we report the effects of prescribed fire on runoff, soil erosion, and rill hydraulics and compare WEPP estimated erosion for several modeling options with measured erosion.

Published by Elsevier B.V.

*Keywords:* WEPP; Rill erosion; Darcy–Weisbach roughness; Shear stress; Rill erodibility; Rill width

### 1. Introduction

The effects of fire on the risk of runoff and erosion can be significant in steep sagebrush rangelands until ground and canopy cover recover. The consequence of fire on runoff and erosion will depend on the weather pattern during the recovery period. Current trends in soil erosion modeling under various management scenarios (including fire) consist of analyzing erosion in probabilistic terms to account for storm variability which requires accurate event-based erosion estimates (Elliot et al., 2001; O’Dea and Guertin, 2003). Under this probabilistic paradigm, it is not

sufficient if a model significantly underestimates large events or overestimates small events, but does well for long-term averages. The physically based Water Erosion Prediction Project (WEPP) model (Nearing et al., 1989; Flanagan et al., 1995) provides event-based erosion estimates and is used to estimate exceedance probabilities for erosion following fire (Robichaud et al., 2005).

Soto and Díaz-Fierros (1998) measured runoff and erosion from natural rainfall on burned and non-burned plots with similar vegetation, slopes and soil textures on gorse (*Ulex europaeus*) shrublands in northwest Spain over a 4-year period. Total runoff from the burned plots was 69% greater than from non-burned plots during the 4-year study. Measured erosion was significantly higher from the burned area than from the control during the first 2 years after fire. In a rainfall simulation experiment, Johansen et al. (2001) reported that erosion and runoff increased due to wildfire on loamy, 5% slope rangelands in New Mexico. Erosion increased by a factor of 25 while runoff

\* Corresponding author.

E-mail addresses: [cmoffet@pw.ars.usda.gov](mailto:cmoffet@pw.ars.usda.gov) (C.A. Moffet), [fperson@nwrc.ars.usda.gov](mailto:fperson@nwrc.ars.usda.gov) (F.B. Pierson), [probichaud@fs.fed.us](mailto:probichaud@fs.fed.us) (P.R. Robichaud), [ken.spaeth@ftw.nrcs.usda.gov](mailto:ken.spaeth@ftw.nrcs.usda.gov) (K.E. Spaeth), [shardegr@nwrc.ars.usda.gov](mailto:shardegr@nwrc.ars.usda.gov) (S.P. Hardegee).

increased by a factor of 2. In Arizona, on a gravelly loam soil (1 to 3% slope) O'Dea and Guertin (2003) reported smaller fire effects on erosion (increased by a factor of 1.4) with similar effects on runoff.

Soto and Díaz-Fierros (1998) compared measured and WEPP estimated soil water content, runoff, and erosion on burned and non-burned sites. Their comparisons excluded events during May through September when the soil was dry and water repellent. They reported that WEPP did reasonably well at predicting runoff and erosion values; although, they reported that on severely burned areas, erosion estimates were consistently underestimated. In one erosion measurement period (6 to 10 months post-burning), WEPP grossly underestimated erosion for control and prescribed burn plots. They attributed this to one large rainfall event (50.3 mm) when water repellency was severe. Soto and Díaz-Fierros (1998, p. 268) concluded, “the model shows a clear tendency to underestimate erosion following severe burns.”

The objectives of this paper were to: (1) evaluate differences in runoff and erosion on a steep mountain big sagebrush (*Artemisia tridentata* ssp. *Vaseyana*) community between burned and non-burned conditions; (2) test the capability of rangeland WEPP for estimating runoff and erosion for burned and non-burned conditions; and (3) suggest model improvement in rangeland WEPP to better represent fire effects on rangelands.

## 2. Theory

The WEPP model treats interrill and rill erosion as separate processes (Nearing et al., 1989). Under the rangeland option in WEPP, interrill erosion is computed as a function of soil interrill erodibility ( $K_i$  adjusted for canopy and ground cover in the interrill area), effective rainfall intensity, interrill runoff rate, and runoff duration (Foster, 1982; Foster et al., 1995). Interrill erosion on undisturbed rangeland has been well studied and is typically low (Hester et al., 1997; Pierson et al., 2001, 2002b; Moffet et al., 2005).

In WEPP, rill erosion is a function of rill detachment capacity, sediment load, transport capacity, rill width, runoff duration, and rill spacing. Rill detachment capacity is modeled as a function of excess soil shear stress (Foster, 1982; Nearing et al., 1989; Foster et al., 1995):

$$D_{rc} = \begin{cases} K_r(\tau_f - \tau_c) & : \tau_f > \tau_c \\ 0 & : \tau_f \leq \tau_c \end{cases} \quad (1)$$

where  $D_{rc}$  is the rill detachment capacity ( $\text{kg m}^{-2} \text{s}^{-1}$ ),  $\tau_f$  is the soil shear stress due to rill flow (Pa),  $\tau_c$  is the critical soil shear stress (Pa) that is required for detachment initiation, and  $K_r$  is the rill erodibility ( $\text{s m}^{-1}$ ). The rill detachment rate ( $D_r$ ,  $\text{kg m}^{-2} \text{s}^{-1}$ ) is equal to rill detachment capacity for clear water flow, but as sediment load ( $G$ ,  $\text{kg m}^{-1} \text{s}^{-1}$ ) approaches the sediment transport capacity ( $T_c$ ,  $\text{kg m}^{-1} \text{s}^{-1}$ ),  $D_r$  approaches 0:

$$D_r = D_{rc} \left( 1 - \frac{G}{T_c} \right) \quad (2)$$

where

$$T_c = k_t \tau_f^{3/2} \quad (3)$$

The adjusted transport coefficient ( $k_t$ ,  $\text{m}^{0.5} \text{s}^2 \text{kg}^{-0.5}$ ) is computed as a function of soil particle characteristics and soil shear stress using a modification of the Yalin (1963) equation as described by Foster (1982). Further adjustment, is made to  $k_t$  for sandy soils by the adjustment factor,  $k_{adj}$  (Foster et al., 1995). On soils with surface sand content less than or equal to 50%  $k_{adj} = 1$  and above 50%  $k_{adj}$  decreases with increasing sand content.

The cumulative rill detachment (kg) from a hillslope segment with net soil loss is

$$E_r = D_r w l t_{RO} \left( \frac{w_h}{w_r} \right) \quad (4)$$

where  $w$  is the rill width (m),  $l$  is the segment length (m),  $t_{RO}$  is the effective runoff duration (s),  $w_h$  is the hillslope width (m), and  $w_r$  is the rill spacing (width between rill centers, m). Each overland flow element (OFE), a section of hillslope with similar soil and management, is divided into 100 slope segments.

The values for  $K_r$  and  $\tau_c$  are WEPP input parameters. In rangeland WEPP these parameters are determined from soil properties and are only adjusted for freezing and thawing effects. Rill soil shear stress,  $\tau_r$ , is a function of ground cover and soil surface characteristics, slope, and rill flow characteristics:

$$\tau_r = \gamma R_h \sin(\tan^{-1}(S)) \left( \frac{f_s}{f_t} \right) \quad (5)$$

where  $\gamma$  is the specific weight of water ( $9807 \text{ N m}^{-3}$ ),  $R_h$  is the hydraulic radius of the rill flow (m),  $S$  is the slope of the energy gradient (assumed equal to the soil surface slope, fraction  $\text{m m}^{-1}$ ),  $f_s$  is the Darcy–Weisbach roughness coefficient due to soil grains (assumed to be 1.11), and  $f_t$  is the total Darcy–Weisbach roughness coefficient due to soil grains, rill area ground cover (litter, rock, plant bases, and cryptogams), and random roughness. In rangeland WEPP,  $f_t$  is empirically estimated from ground cover and random roughness parameters, but under uniform flow conditions the definition is

$$f_t = \frac{8gR_h S}{V^2} \quad (6)$$

where  $g$  is the acceleration due to gravity ( $9.807 \text{ m s}^{-2}$ ) and  $V$  is the mean flow velocity ( $\text{m s}^{-1}$ ).

The rill hydraulic radius ( $R_h$ ) is computed assuming a rectangular cross-section as functions of width ( $w$ ) and depth ( $d$ ). In WEPP, width is a function of rill discharge ( $q$ ,  $\text{m}^3 \text{s}^{-1}$ ) (Gilley et al., 1990):

$$w = a q^b \quad (7)$$

where  $a = 1.13$  and  $b = 0.303$ . Given the rill discharge, slope, width, and Darcy–Weisbach roughness coefficient, depth is computed by WEPP as

$$d = \frac{\left( \frac{q}{C\sqrt{S}} \right)^{2/3} (w + 2d)^{1/3}}{w} \quad (8)$$

where  $C$  is the Chezy discharge coefficient ( $C = \sqrt{8g/f_t}$ ).

For a given storm, infiltration is affected by the effective hydraulic conductivity ( $K_e$ ) and the matric potential gradient across the wetting front. Roughness ( $f_i$ ) does not influence infiltration in the model: however, peak discharge ( $q_p$ ), and runoff duration ( $t_{RO}$ ) are sensitive to  $f_i$ . As  $f_i$  increases,  $q_p$  decreases and  $t_{RO}$  increases.

For a given discharge, the excess soil shear stress computed by WEPP is a function of only one factor affected by management—the Darcy–Weisbach roughness coefficient. In the current version of WEPP, any effect of management (excluding freezing and thawing effects) on estimated rill erosion must be expressed through differences in erodibility, runoff, and Darcy–Weisbach roughness coefficients.

### 3. Materials and methods

The study area is located at the Reynolds Creek Experimental Watershed in southwest Idaho near the divide between Reynolds Creek and Dobson Creek watersheds (43° 6' 30" N; 116° 46' 50" W). The elevation of the research site is about 1750 m and mean annual precipitation is approximately 592 mm (1965–1975).

The vegetation before the prescribed burn was a typical mountain big sagebrush community with subdominant shrubs of rabbitbrush (*Chrysothamnus viscidiflorus*), antelope bitterbrush (*Purshia tridentata*), and widely scattered juniper (*Juniperus occidentalis*). Dominant grasses were bluebunch wheatgrass (*Pseudoroegneria spicata*) and Idaho fescue (*Festuca idahoensis*). The soils are mapped Kanlee–Ola–Quicksilver association, 3 to 50% slopes (Harkness, 1998). All plots in this study were on the deeper Kanlee (fine-loamy, mixed, superactive, frigid Typic Argixerolls) and Ola (coarse-loamy, mixed, superactive, frigid Pachic Haploxerolls) series. The slopes of the study area were 35 to 50% with an east facing aspect on granite bedrock hillslopes. Soil textures were coarse sandy loam in the surface 30 cm and loam or coarse sandy loam in the subsoil that extends beyond 100 cm depth. Rock fragment (>2 mm diameter) content in the surface layer was about 5 to 15% and ranged between 5 and 50% in the subsoil. Soil water content during all phases of this research was low (approximately 0.03 kg kg<sup>-1</sup>).

#### 3.1. Large plot rainfall simulations

Sixteen rectangular plots (6.5 m long by 5 m wide) were selected within a narrow elevation band near the top of the hillslope prior to prescribed fire. Eight plots each were assigned to the non-burned and burned treatments. Plots in the non-burned treatment were characterized (canopy and ground cover, slope, and random roughness) and rainfall simulations were performed in August and early September. The prescribed fire was ignited in late September and a head fire burned the study area. The burned plots were characterized and simulated rainfall was applied in October.

Rainfall was applied on two plots each day with a Colorado State University type rainfall simulator (Holland, 1969) at an average rate of 60 mm h<sup>-1</sup> for 1 h; however, observed application

rates differed from the design due to mechanical difficulties and wind. The observed range among plots was 45 to 76 mm. Several samples of rainfall that fell directly in the runoff collection trough were collected during the first several minutes of each simulation. Timed samples (500 ml to 1000 ml) were collected approximately every minute. Sediment mass and water volume collected from each sample were determined in the laboratory. The mean trough catch that would have been collected during the sample time was subtracted from each sample volume.

Vegetation cover, ground cover, slope, and surface random roughness were sampled in each large plot prior to the rainfall simulations with one hundred evenly spaced point samples recorded along six horizontal transects (0.5, 1.5, 2.5, 3.5, 4.5, and 5.5 m from the upslope end of a plot). At each point the relative elevation of the ground surface (measured to the nearest mm), the ground cover class, and the canopy cover class (if present) were recorded. Vegetation and litter mass were determined by harvesting all standing plant material by functional group and collecting litter from 30 small (1 m<sup>2</sup>) plots nearby. The vegetation and litter samples were oven dried and weighed.

Random roughness was computed by first performing loess regressions (Cleveland, 1979) on each transect between relative elevation and distance along the transect, using a span parameter of 0.2 (approximately a 1-m window). For each transect, the residual standard deviations were computed. The random roughness for the plot is the mean of the six standard deviations for each transect.

#### 3.2. Rill experiments

Rill erosion experiments were conducted on the large plots used in the rainfall simulation experiments within 6 h after the rainfall simulations were completed. A flow regulator fitted with a Styrofoam peanut-filled box energy dissipater was used to apply water through a 10-cm wide opening. The water was released 4 m upslope of the runoff collection troughs. The regulator was sequentially adjusted to apply inflow rates of 3, 7, 12, 13, 21, and 24 l min<sup>-1</sup> for 12 min each. At each inflow rate, 6 to 11 timed outflow samples (500 or 1000 ml) were collected and sediment yield and discharge were determined. Samples were classified as “early” if the sample was collected less than 6 min after the start of an inflow rate and “late” otherwise. A total of 433 samples were collected during the rill experiments. Rill width and depth were measured at several (3 to 7) transects along the slope during each inflow rate. The mean of all available transects during each inflow rate was calculated and used in the analysis. Conductivity probes were positioned in the primary flow path at 1 and 3 m from the upslope end of the rill. The conductivity of the water was sampled 8 times each second at each probe while a small (approx. 50 ml) pulse of CaCl<sub>2</sub> solution flowed in the rill. The difference in time between the maximum conductivity readings on each probe was recorded.

The rill detachment capacities used in regression analyses to compute  $K_r$  were estimated as described by Elliot et al. (1989), Eq. (9). Since there were no interrill sediment additions to the rills, the rill detachment capacity equation is reduced to:

$$D_{rc} = \frac{-T_c}{l} \ln \left[ 1 - \left( \frac{Q_s}{wT_c} \right) \right] \quad (9)$$

Table 1  
WEPP estimated soil particle size characteristics for Kanlee surface soil

Diameter (mm)	Specific gravity (kg m <sup>-3</sup> )	Mass fraction (kg kg <sup>-1</sup> )
0.002	2.60	0.057
0.010	2.65	0.031
0.030	1.80	0.204
0.436	1.60	0.548
0.200	2.65	0.160

where  $Q_s$  (kg s<sup>-1</sup>) is the sediment discharge. The adjusted transport coefficient ( $k_t$ ) used to compute  $T_c$  was calculated using the modified Yalin (1963) equation from WEPP estimated sediment particle size characteristics and a soil shear stress of 8 Pa (Table 1). Sediment particle size characteristic estimates were based on surface Kanlee soil characteristics (sand 60.4%, clay 15.3%, organic matter 3%, and  $k_{adj}=0.4904$ ). The transport capacity was computed for each sample using Eq. (3).

Detachment capacity is undefined when  $Q_s \geq wT_c$ . The few samples (approx. 10%) meeting this condition were excluded from the analysis.

The surface area used to compute  $D_{rc}$  was based on measured rill width rather than WEPP estimated rill width. The estimated soil shear stress,  $\tau_f$ , was computed as in Eq. (5). The values of  $R_h$  and  $f_t$  were based on mean measured rill width, mean rill discharge, slope, and mean measured rill flow velocity for each inflow rate. The value of  $R_h$  was calculated from measured rill width and the best estimate of depth,  $d$  (estimated by assuming a rectangular rill cross-section and dividing cross-sectional area,  $A=q/V$ , by  $w$ ). The value of  $f_t$  was computed as in Eq. (6).

Rill erodibility was computed for each plot by regression of estimated rill detachment capacity,  $D_{rc}$ , on estimated soil shear stress,  $\tau_f$ , and deriving the regression estimates  $\beta_0$  and  $\beta_1$ . Rill erodibility is  $\beta_1$ . Critical shear stress was calculated as

$$\tau_c = \frac{-\beta_0}{\beta_1}. \quad (10)$$

If  $\beta_0$  was estimated greater than 0 (incorrectly indicating  $D_{rc} > 0$  when  $\tau_f = 0$  or that  $D_{rc}$  decreases with increasing  $\tau_f$ ) then the regression analysis was recomputed removing the intercept term from the model. Removing the intercept term forces  $\tau_c = 0$  and  $K_r > 0$ .

### 3.3. WEPP modeling schemes

The modeling approach used was designed primarily to investigate the rill erosion process in WEPP. Five parameterization schemes were used to explore the WEPP rill erosion estimation capabilities (Table 2). As shown in Eqs. (1) and (5) rill detachment capacity is a function of two erodibility terms ( $K_r$  and  $\tau_c$ ) and four terms related to the erosivity of the concentrated flow ( $R_h$ ,  $S$ ,  $f_s$  and  $f_t$ ). Of these four terms,  $R_h$  and  $f_t$  are estimated by WEPP based on rill area ground cover, random roughness, peak runoff, slope, and two width–discharge parameters. The rill experiments demonstrate that measured values for these two terms were poorly correlated

with WEPP estimates. The parameterization options are a progression of replacing WEPP estimated values with measured values for a series of these terms to determine the effect these terms have on the erosion prediction.

The first parameterization scheme (Option A) was selected to test how well rangeland WEPP predicts rill erosion utilizing data available to typical model users, given that total runoff was correctly estimated. Since this study was primarily interested in exploring the rill erosion process it was necessary that runoff be estimated correctly. To achieve this,  $K_e$  was optimized on total runoff. The fundamental parameters that users adjust to influence rill erosion are  $K_r$  and  $\tau_c$ . Measured values from the rill experiments were used in Option B. Option C replaces WEPP estimated rill area Darcy–Weisbach roughness coefficients ( $f_t$ ) with measured values for each treatment from the rill experiments. This was achieved by replacing measured rill area ground cover and random roughness values with values that yielded the measured  $f_t$  values. The  $R_h$  and  $f_t$  terms are not independent (see Eq. (8)), so adjusting  $f_t$  in Option C also had an effect on  $R_h$ . Option D directly addresses  $R_h$  by altering the width–discharge relationship in WEPP to match the relationship found for each treatment from the rill experiments. In Option E,  $K_r$  and  $\tau_c$  parameters were optimized on total erosion to determine if WEPP could be parameterized to match the measured large plot erosion in each plot.

In all scenarios the soil data were those available in the 1995 WEPP soils database for Kanlee soil. Soil saturation was always adjusted to 25% (about 8% gravimetric water content), and effective hydraulic conductivity and rill erodibility were adjusted as described above. The management data were written to run WEPP for rangelands in event mode. Measured canopy cover, rill and interrill ground cover (litter, plant base, cryptogam, and rock), and random roughness were used to parameterize the initial condition section for each plot except in Options C through E as indicated above. In all cases, a rill spacing of 1 m was selected. About 5 rills were observed exiting each plot during the rainfall simulations. Precipitation data were based on the measured simulated rainfall on each plot. Pattern parameters were assumed to be the same on all plots (duration

Table 2  
Description of the five model parameterization schemes used in this study

Option	Description
A	Used readily available soil and cover data; $K_r$ , $K_e$ , and $\tau_c$ computed by WEPP, but $K_e$ was optimized on total measured runoff for each plot to eliminate differences between measured and modeled runoff as a source of error in the erosion prediction.
B	As in A, but rill erodibility ( $K_r$ ) and critical shear ( $\tau_c$ ) values were replaced with treatment specific $K_r$ and ( $\tau_c$ ) values measured during the early period of the rill experiments.
C	As in B, but random roughness and rill ground cover (WEPP's rough, resr, rokr, basr, and cryr) were adjusted so that the total WEPP-computed Darcy–Weisbach roughness coefficients in the rill area ( $f_t$ ) matched the treatment mean $f_t$ from the rill experiments.
D	As in C, but rill width equations were modified in WEPP to match the treatment specific width–discharge relationships from the rill experiments.
E	As in D, but $K_r$ values were optimized on measured sediment yield given $\tau_c = 0.0001$ .

of 1 h, peak intensity of 1.01 times the mean intensity, and time to peak intensity at 20% of the simulation duration).

### 3.4. Statistical analysis

One-way analysis of variance was used to test the significance of treatment effects on response variables for the large plot rainfall simulation experiments. Since only two treatment levels were studied, a significant *F*-test indicated that the means were different. Welch's *t*-test was used within each treatment to compare WEPP estimated with measured runoff and erosion for each of the parameterization schemes.

Analysis of variance was used to test the effect of burning on width versus discharge relationship parameters. Analysis of variance was also used to test whether the parameters were different from those determined by Gilley et al. (1990).

Linear regression analysis was used to derive relationships between Darcy–Weisbach roughness coefficients and mean rill flow rate for each treatment. Analysis of variance was used to test the significance of the differences in regression-estimated parameters between the treatments and with those proposed by Gilley et al. (1990).

Analysis of variance was used to test for burn treatment and period effects on estimated  $K_r$ . Prior to this analysis, the  $K_r$  values were log transformed by  $\ln(K_r+0.0001)$  to address deviations from normality (Neter et al., 1996). A linear mixed-effects model was fit considering the intercept as a random effect and burn treatment and sample period were considered fixed effects.  $K_r$  estimates from this analysis were back-transformed to its original units for reporting and for use in the WEPP model.

## 4. Results and discussion

### 4.1. Plot and simulation characteristics

Total precipitation applied and plot slope were similar for burned and non-burned treatments (Table 3). On burned plots, almost no standing material remained, except occasional bitterbrush shrub skeletons (sagebrush was consumed to within 5 cm of the soil surface). Average canopy cover of the shrub skeletons was 0.2% (Table 3).

The burn treatment significantly reduced total litter, plant basal cover and canopy cover (Table 3). Between plant canopy litter cover (ashy unconsumed litter and wood) was not different between burned and non-burned treatments even though total litter cover was reduced by fire. This was because the total areas outside the canopy significantly increased following the fire. Random roughness was significantly less in burned than in non-burned plots (Table 3). This was likely due to root crowns and litter under shrubs being consumed during the fire. The burned plots had greater rock cover compared to the non-burned plots (Table 3). However, a 0.5% increase in rock cover in burned plots probably had little or no effect on hillslope hydrological or erosion responses.

Mass of litter and vegetation was reduced by fire (Table 3). Litter accumulation, including dung and wood accounted for

Table 3

Comparison of site and simulation characteristics between burned and non-burned treatments

Characteristic (units)	Burned	Non-burned
Precipitation (mm)	59.1 a	61.4 a
Slope (%)	41.6 a	40.8 a
Random roughness (mm)	10.8 b	21.1 a
Ground cover <sup>a</sup>		
Litter below canopy (%)	0.1 b	49.6 a
Rock below canopy (%)	0.0 a	0.1 a
Basal below canopy (%)	0.0 b	1.3 a
Litter between canopy (%)	23.3 a	24.7 a
Rock between canopy (%)	1.0 a	0.3 b
Basal between canopy (%)	0.0 b	0.6 a
Canopy cover (%)	0.2 b	57.0 a
Litter total (%)	23.4 b	74.3 a
Rock total (%)	1.0 a	0.5 b
Basal cover total (%)	0.0 b	1.9 a
Bare ground total (%)	75.6 a	24.3 b
Ground litter (kg ha <sup>-1</sup> )	808 <sup>b</sup>	9517
Vegetation (kg ha <sup>-1</sup> )	– <sup>c</sup>	12,125

Means ( $n=8$ ) for a characteristic followed by the same letter are not significantly different ( $\alpha=0.05$ ).

<sup>a</sup> The sum of litter, rock, and basal cover below canopy and outside canopy and total bare ground is equal to 100.

<sup>b</sup> Burned treatment litter samples were collected in the spring and early summer following the fire.

<sup>c</sup> Burned treatment vegetation samples were not collected.

nearly 45% of the total mass of above ground organic matter. Litter in non-burned plots was not uniformly distributed on the ground, but rather occurred as a thick almost continuous layer under canopies and patchy thin accumulations outside canopies. The litter mass in burned plots was 8% of that in non-burned plots, but total litter cover on the burned treatment was 31% of that on the non-burned treatment. The relative effect of fire on litter cover was less than on litter mass/volume. This result is similar to that found by others (Soto and Díaz-Fierros, 1998; Pierson et al., 2002a). Soto and Díaz-Fierros (1998) reported litter mass was 19% of the non-burned plot, but rill and interrill ground cover were 50% of the non-burned 1 year after fire. Pierson et al. (2002a) reported much greater loss of both mass and cover from a wildfire in Nevada, but the proportion of mass removed due to fire was greater than the proportion of cover removed.

### 4.2. Measured large plot runoff and erosion

Fire significantly increased total runoff volume ( $\alpha=0.05$ ) from burned plots (16.6 mm, SE=3.04 mm,  $n=8$ ) compared to non-burned plots (3.0 mm, SE=1.53 mm,  $n=8$ ). All burned plots yielded runoff, while three of the eight non-burned plots yielded no runoff. This is consistent with findings from Soto and Díaz-Fierros (1998), Johansen et al. (2001) and O'Dea and Guertin (2003). Soto and Díaz-Fierros (1998) found that wet-season runoff doubled in the first year after fire.

One partial explanation for the greater runoff from the burned plots is that canopy interception capacity was reduced. Soto and Díaz-Fierros (1997) reported the canopy of non-burned plots had a maximum predicted 1-day interception loss of 8.7 mm and 2.5 mm for burned plots the first year after fire.

Using these values as inputs to Calder's (1986) interception model the difference in interception for a 60-mm precipitation event is just over 6 mm.

Burned areas generated runoff more quickly than non-burned areas. The mean time to initiation of runoff for burned and non-burned plots was 3.27 min (SE=0.66 min,  $n=8$ ) and 7.08 min (SE=1.23 min,  $n=5$ ), respectively. Peak runoff rates from burned plots were about three times higher than the non-burned plots (all non-burned plots) and about two times greater than the five non-burned plots with measurable runoff (Fig. 1). Regardless of treatment, runoff rates peaked 10 to 20 min into the simulated rainfall event and diminished with time thereafter (Fig. 1). The decrease in runoff rate with time during the simulation, for both burned and non-burned plots, indicates that the soil in both treatments may have water repellent soil properties. Pierson et al. (2001) found significant water repellency in both burned and non-burned plots for similar sites during late summer and early fall when the soils were dry. The effect of fire on water repellency index was greatest in the coppice micro-site (Pierson et al., 2001). Soto and Díaz-Fierros (1998) reported that runoff to precipitation ratios for natural rainfall on control and burned plot, were significantly greater during periods of high water repellency.

The effect of burning on total soil erosion was significant ( $\alpha=0.05$ ). Sediment yield for burned plots was  $10.7 \text{ Mg ha}^{-1}$  (SE=2.37  $\text{Mg ha}^{-1}$ ,  $n=8$ ) and  $0.1 \text{ Mg ha}^{-1}$  (SE=0.06  $\text{Mg ha}^{-1}$ ,  $n=8$ ) for the non-burned plots. Erosion rates in both burned and non-burned treatments were greatest during the first 7 to 20 min of the simulated rainfall event and steadily decreased thereafter (Fig. 2). Soto and Díaz-Fierros (1998) reported that erosion was higher in burned compared to control plots the first 2 years post-fire. In one erosion measurement period, when almost all erosion occurred from one 50.3 mm

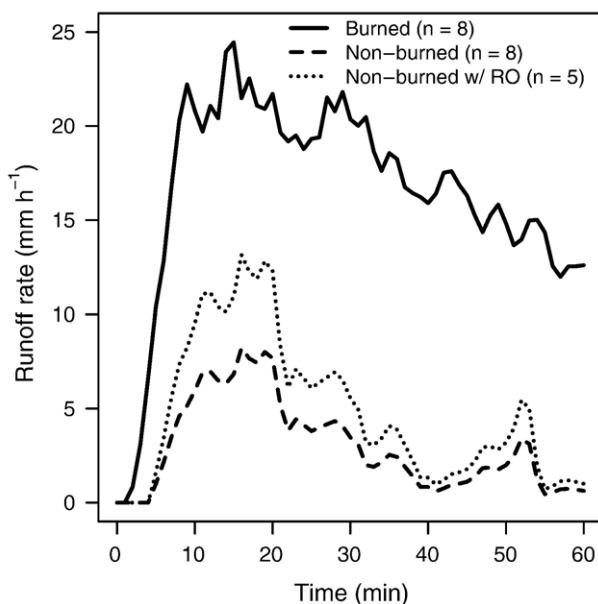


Fig. 1. Mean hydrographs for 60-minute simulated rainfalls on burned and non-burned plots ( $n=8$ ). Three non-burned plots yielded no runoff and the mean hydrograph for the five plots that did generate runoff is also shown ( $n=5$ ).

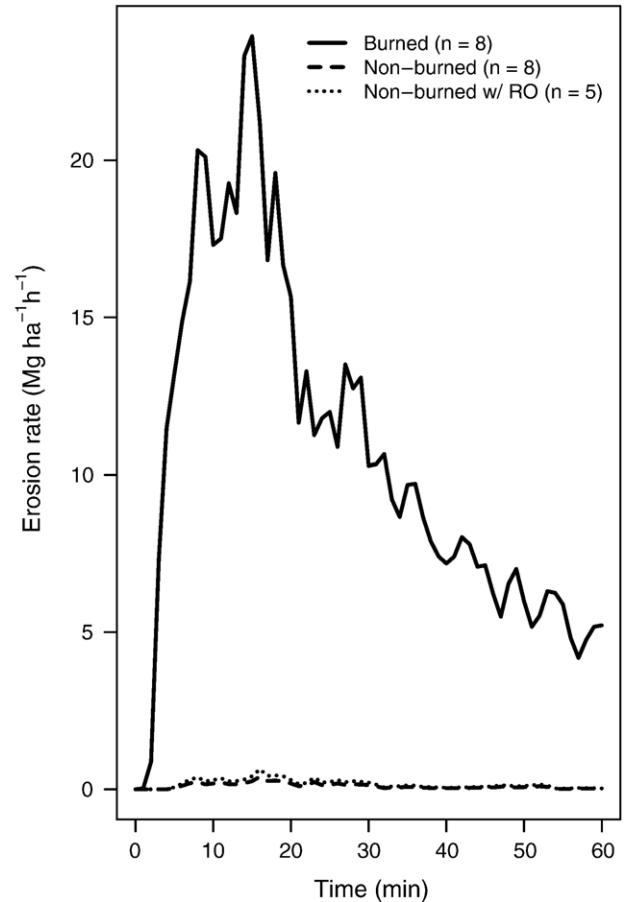


Fig. 2. Mean sediment yield for 60-minute simulated rainfalls on burned and non-burned plots ( $n=8$ ). Three non-burned plots yielded no runoff or sediment and the mean sediment yield response for the five plots that did generate runoff is also shown ( $n=5$ ).

storm on dry water repellent soils, erosion was 6.6 times greater from burned plots than from control plots (Soto and Díaz-Fierros, 1998). Pierson et al. (2001) reported that significant increases in interrill erosion from rainfall simulation experiments were limited to the first year after fire and only in the coppice micro-site.

#### 4.3. Measured rills

In the rill analysis we compared rill hydraulic characteristics and rill detachment rates between treatments. Measured rill width and rill flow data were used to develop treatment specific width versus discharge parameters. In addition to the treatment effects on rill erodibility, early and late period samples were compared to determine if rill erodibility was static during the experiment.

##### 4.3.1. Rill width

Mean rill width for the burned plots was 0.195 m (SE=0.022 m,  $n=8$ ), but the non-burned plots mean was 0.259 m (SE=0.043 m,  $n=8$ ). Width in each treatment was a function of mean rill flow rate (Fig. 3). In general, the burned plots had rill widths that were narrower than the non-burned plots for the same rill flow rate.

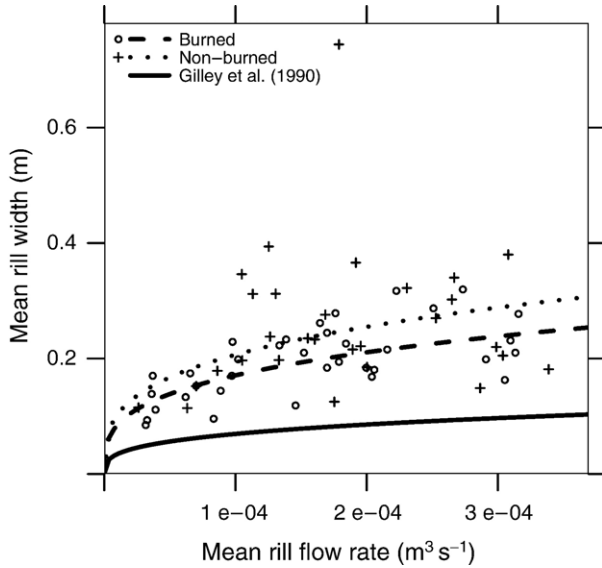


Fig. 3. Rill width versus mean rill flow rate for the burned and non-burned plots. Curves are regression estimates for the burned, non-burned, and current WEPP equation from Gilley et al. (1990).

Regardless of treatment, the measured rill widths were wider than would be computed by WEPP for most of the discharge range. Wider than typical rills have been observed on cropland once the soil was eroded to a non-erodible consolidated boundary below the surface (Foster, 1982). Regression analysis using the  $\ln(w) = \ln(a) + b \ln(q)$  functional form (Eq. (7)) showed that  $b$  was not significantly different ( $\alpha=0.05$ ) from Gilley et al. (1990), regardless of treatment. However,  $\ln(a)$  was significantly different from that of Gilley et al. (1990). Estimated  $\ln(a)$ , given a fixed  $b$  value, was significantly different ( $\alpha=0.05$ ) between treatments:

$$w = 2.783q^{0.303} \tag{11}$$

for burned plots and

$$w = 3.366q^{0.303} \tag{12}$$

for non-burned plots (Fig. 3).

The Gilley et al. (1990) rill width–discharge relationship was developed from cropland sites that were moldboard-plowed 3 to 12 months before and disked immediately prior to the tests. The soil erodibility characteristics within the tillage zone were relatively uniform during the test and non-erodible boundaries were not reached. In this study, no tillage was performed at any time prior to the tests and a less erodible layer was encountered below the very near surface soil which may explain the greater widths observed.

#### 4.3.2. Hydraulic roughness

The mean WEPP estimated Darcy–Weisbach roughness coefficients were more similar between treatments than were measured (Table 4). The Darcy–Weisbach roughness coefficient was a function of discharge for the non-burned treatment (Fig. 4), but theoretically this term should be independent of flow. Darcy–Weisbach roughness coefficient estimates from

Table 4  
Mean WEPP estimated and optimized runoff and erosion parameters for burned and non-burned treatments ( $n=8$ )

Parameter (units)	Burned	Non-burned
<i>Mean WEPP values</i>		
$K_{i,adj}^a$ ( $\text{kg s m}^{-4} \times 10^{-6}$ )	0.3470	0.0001
$K_r$ ( $\text{s m}^{-1} \times 10^3$ )	0.629	0.629
$\tau_c$ (Pa)	0.939	0.939
$f_i$ (NOD)	10.99	22.27
$a$ (NOD)	1.13	1.13
<i>Experimentally estimated values</i>		
$K_r$ ( $\text{s m}^{-1} \times 10^3$ )	3.222	0.353
$\tau_c$ (Pa)	0.366	0.366
$f_i$ (NOD)	7.159	28.54
$a$ (NOD)	2.783	3.366
<i>Mean optimized values</i>		
$K_c$ ( $\text{mm h}^{-1}$ )	20.59	40.00
$K_r$ ( $\text{s m}^{-1} \times 10^3$ )	43.000	0.963 <sup>b</sup>
$\tau_c$ (Pa)	0.0001	0.0001

<sup>a</sup> Adjusted interrill erodibility.

<sup>b</sup> Mean of the five non-burned plots with runoff.

WEPP are a function of ground cover and do not vary with discharge.

The patchy nature of litter cover and cover depth in the non-burned plots may explain the variation in hydraulic roughness with discharge. As flow increases, depth of flow increases, causing more of the flow to extend above roughness elements. At low flow, the flow is confined within the litter layer (i.e., porous flow). Based on this theory, hydraulic roughness would decrease with increasing rill flow depth to a point at which all the litter is submerged and hydraulic roughness would remain constant for greater flow depths. Recall that litter was greatly reduced by burning in terms of cover and mass/volume (Table 3). This

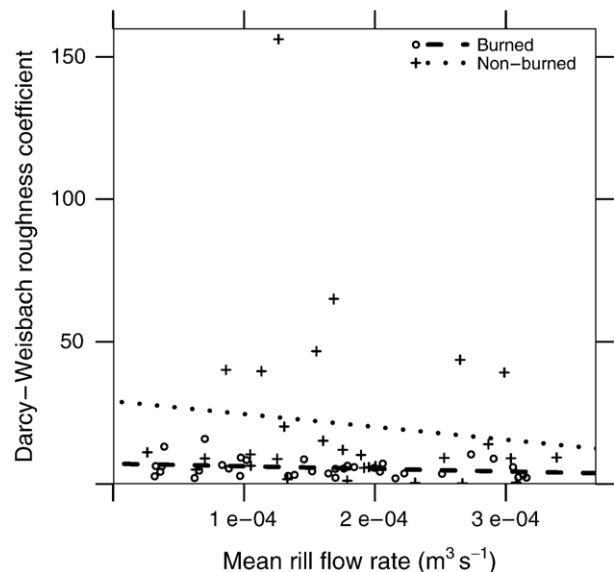


Fig. 4. Darcy–Weisbach roughness coefficients versus mean rill flow rate for the burned and non-burned plots. Lines are regression estimates for the burned and non-burned data.

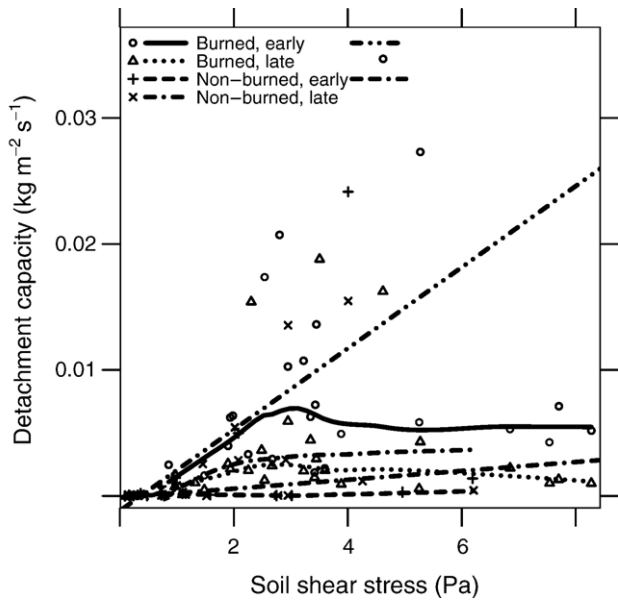


Fig. 5. Detachment capacity versus soil shear stress for burned and non-burned plots during early and late periods of each inflow rate. The 4 curves (left side of legend) are loess regression predictions and the 2 lines (right side of legend) are simple linear regression predictions (theoretical functional form of WEPP). Note: One burned early point at  $D_{rc}=0.0745$  and  $\tau_r=2.487$  is not shown in the figure but the value was used in the analysis.

reduced litter on burned plots resulted in less litter–flow interaction and the litter was fully submerged over the range of flow studied.

### 4.3.3. Rill erodibility

Regression analyses of rill detachment capacity versus soil shear stress were performed as in Eq. (1) separately using early and late period samples. Among the 15 burned analyses, only 6

showed both  $K_r$  and  $\tau_c$  to be positive. Among the 12 non-burned analyses, 7 showed detachment capacity–soil shear stress relationships that were supportive of rill detachment theory (i.e., positive  $K_r$  and  $\tau_c$ ). For the 14 detachment capacity–soil shear stress regressions with negative  $\tau_c$  or  $K_r$ , the  $\tau_c$  was fixed at 0 ensuring that  $K_r$  was positive. The overall means of  $K_r$  and  $\tau_c$  from all 27 regression analyses were  $0.002739 \text{ s m}^{-1}$  and  $0.366 \text{ Pa}$ , respectively.

Separating out early and late samples showed that rill detachment capacity decreased with time during a 12-min flow rate period (Fig. 5). When the flow was increased, detachment would increase for the first several minutes of the new inflow rate then tail off to a lower detachment rate. In the burned treatment,  $K_r$  estimates for early samples were significantly greater than for late samples ( $0.003222 \text{ s m}^{-1}$  versus  $0.001018 \text{ s m}^{-1}$ ), but in the non-burned treatment the  $K_r$  estimates were less for the early samples than for the late samples ( $0.000353 \text{ s m}^{-1}$  versus  $0.000446 \text{ s m}^{-1}$ ). Estimates of  $\tau_c$  were statistically similar regardless of sample time or treatment (burned early=0.62, burned late=0.20, non-burned early=0.49, and non-burned late=0.16).

Loess regression, a method developed by Cleveland (1979) to explore the shape of regression functions, was performed for each treatment–period combination with a span parameter of 0.6 (60% of the data considered in a local window) This method frees the analyst from having to specify the correct functional form of the relationship. The non-linear relationship between detachment capacity and soil shear stress shown in this analysis (Fig. 5) suggests a deficiency in WEPP theory and the method used in collecting these data (i.e.,  $K_r$  is not constant during an event).

Detachment capacity increases with soil shear stress for shear stress values less than 2.5 Pa (Fig. 5). Above this point detachment capacity is insensitive to changes in soil shear stress. Rill

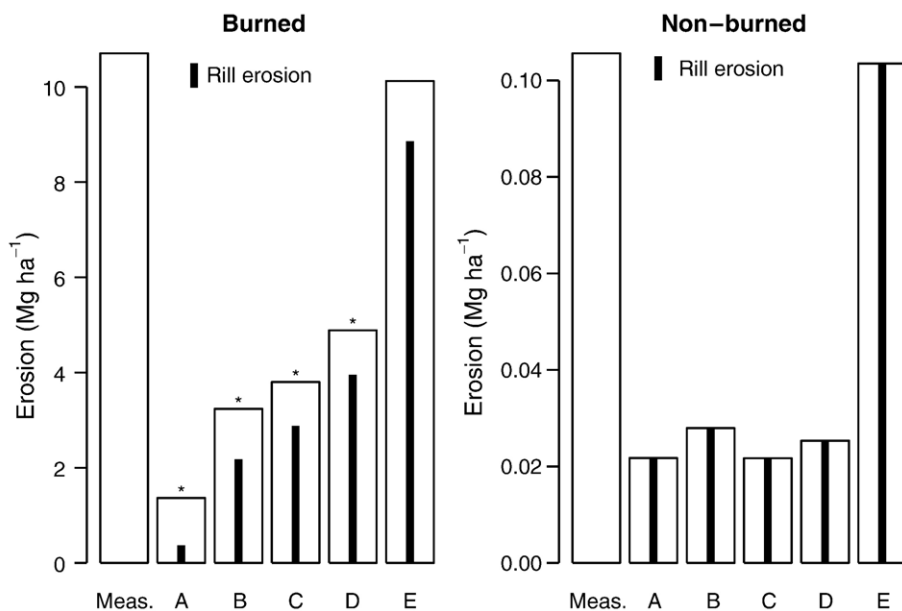


Fig. 6. Mean measured and WEPP estimated erosion for five parameterization options on burned (r) and non-burned (l) plots. Solid vertical lines in the center of each bar are mean WEPP estimated rill erosion. WEPP estimated erosion values within a treatment marked above the bar with an asterisk are significantly different ( $\alpha=0.05$ ) from the mean measured value.



inflow rate (and therefore soil shear stress) was varied monotonically so that at the highest inflow rates some portion of the rill surface area had been subject to shear force for about 1 h. In terms of duration of shear force, early period samples at the highest inflow rates are not equivalent to early period samples at the lowest inflow rates. As the inflow rate was increased, rills widened or flow paths shifted to encompass rill surface area not previously eroded. Rill erodibility is not currently dynamic during runoff events in WEPP. The break in sensitivity to changes in soil shear stress may be related to exhaustion of more erodible material at the surface due to erosion by the lower inflow rates. [Alberts et al. \(1980\)](#) found that rill erosion rate was constant over a 10:1 ratio of highest to lowest flow rate on untilled, consolidated soils. Erosion was significant under these conditions, but the erosion rate was controlled by the soil and was independent of flow hydraulics.

#### 4.4. WEPP estimated runoff and erosion

##### 4.4.1. Option A, optimized $K_e$

By optimizing  $K_e$  values, runoff converged to within 0.4 mm of the measured value for all plots. Mean measured runoff was 16.62 mm and 3.04 mm for the burned and non-burned treatments, respectively. The mean WEPP estimated runoff values for this option were 16.81 mm (burned) and 3.05 mm (non-burned).

Using WEPP estimated erosion parameters predicted erosion was 13% of measured erosion for the burned treatment ([Fig. 6](#)). The erosion estimate for the non-burned treatment was statistically similar at 21% of measured erosion ([Fig. 6](#)). WEPP adequately estimated low erosion for the non-burned condition and showed an increase in erosion due to fire. However, the predicted increase due to fire was only 1.3 Mg ha<sup>-1</sup> compared to a 10.6 Mg ha<sup>-1</sup> measured increase. The increase in WEPP estimated erosion due to fire was predominately due to an increase in interrill erosion ([Fig. 6](#)). [Pierson et al. \(2003\)](#) found that for similar sites rill erosion dominated total sediment yield compared to interrill erosion. Therefore, it was assumed the majority of error in WEPP estimated erosion under Option A was due to error in estimated rill erodibility and perhaps critical shear parameters.

##### 4.4.2. Option B, measured $K_r$ and $\tau_c$

Replacing WEPP estimated  $K_r$  and  $\tau_c$  with measured values increased the erosion estimated for the burned and non-burned plots relative to Option A ([Fig. 6](#)). In the non-burned treatment  $K_r$  was decreased, but erosion still increased since  $\tau_c$  was also significantly reduced. The mean soil shear due to rill flow in non-burned plots was 0.712 which is intermediate to the WEPP estimated and measured critical shears ([Table 4](#)). This explains why the erosion estimate increased in the non-burned treatment when  $K_r$  was decreased. The non-burned plot estimate was still acceptable (i.e., statistically similar to the measured value). The burned plot erosion estimate, at more than double the value in Option A, was still significantly less than that measured ([Fig. 6](#)).

Erosion in the burned treatment may have been underestimated due to a reduction in rill erodibility between the start

of rainfall simulation and the start of rill experiments as much soil was eroded. Alternatively, the underestimation of erosion may be due to erosivity differences between actual and modeled rills. The next two options explore this possibility.

##### 4.4.3. Option C, measured $f_i$

Adjusting the rill area ground cover and random roughness inputs to get Darcy–Weisbach roughness coefficients equal to treatment mean values ([Table 4](#)) had 3 effects. First, this changed how total shear stress was partitioned between soil grains and other sources of roughness (see Eq. (5)). Second, there was a very slight reduction in runoff volume generated (i.e., treatment means were not statistically different from those measured). Third, the routing of flow down the slope and therefore peak runoff was changed.

Decreasing the roughness by 34% for burned plots resulted in a 17% increase in the mean erosion estimate (still significantly less than measured). Increasing the roughness by 28% in the non-burned treatment reduced the erosion estimate by 22% (an almost indiscernible amount in absolute terms) ([Fig. 6](#)). The non-burned erosion estimate was not significantly different from measured erosion.

Mean WEPP estimated total runoff for the burned treatment decreased with this option from 16.81 mm to 16.64 mm which is very similar to the mean measured value of 16.62 mm. The non-burned WEPP estimated runoff decreased from 3.06 mm to 2.89 mm compared with the measured value of 3.04 mm. It is not clear why total runoff decreased in each treatment for this option, but the estimates are reasonably similar to previous option estimates and the measured value. Options D and E produce the same runoff values as this option.

Mean peak runoff decreased in the non-burned treatment from 9.6 mm h<sup>-1</sup> to 7.9 mm h<sup>-1</sup> and decreased very slightly in the burned treatment from 26.6 mm h<sup>-1</sup> to 26.5 mm h<sup>-1</sup>. Based on the WEPP width equation (Eq. (7)), mean burned plot rill width was 8.5 cm regardless of the slight reduction in flow. In the non-burned treatment calculated rill width decreased from 5.0 cm to 4.7 cm as a result of the reduced flow. In each treatment, WEPP estimated rill widths are significantly narrower than those predicted by Eq. (11) (13.4 cm, burned) and Eq. (12) (11.9 cm, non-burned) developed from rill experiments. This discrepancy between measured and WEPP estimated rill width suggests the next option.

##### 4.4.4. Option D, measured $a$

For this study WEPP was modified to compute rill width using the relationships developed from the rill experiments (Eqs. (11) and (12)). Even with the runoff, rill erodibility, critical shear, rill width, and hydraulic roughness adjusted to match measured values erosion was underestimated in the burned treatment ([Fig. 6](#)).

Increasing  $a$  has many effects in the model that influence the erosion estimate. All else being equal, an increase in  $a$  will increase  $w$  (Eq. (7)) and decrease  $d$  (Eq. (8)) and  $R_h$ . A decrease in  $R_h$  will cause a decrease in  $\tau_f$ ,  $D_{rc}$ ,  $T_c$ , and finally  $D_r$  (Eqs. (1–3)). Even though  $D_r$  decreases as  $a$  increases, greater rill width ( $w$ ) exposed to the erosive shear force and available to transport

sediment may result in an increase in predicted erosion. The ultimate effect of changes in  $a$  on erosion estimates will depend on the balance between width subject to erosion/transport and unit width rill detachment rate.

In the non-burned treatment,  $a$  was increased 200% which only resulted in a 17% increase in predicted erosion. In the burned treatment, however,  $a$  was increased only 150% and predicted erosion increased by 29%. In each case the adjustment made to  $a$  resulted in an improved erosion prediction; however, in the burned treatment the magnitude was not sufficient to be considered adequate. These data show that rill width is an important factor in estimating rill erosion. It is important that a physically based model estimates rill width correctly.

#### 4.4.5. Option E, optimized $K_r$

The  $K_r$  values from optimization on total erosion were greater than WEPP estimated values regardless of treatment (Table 4). WEPP estimated and measured erosion converged (within  $0.02 \text{ Mg ha}^{-1}$ ) in five of the eight burned plots. The  $K_r$  values for these five plots ranged from  $1.114 \times 10^{-3}$  to  $17.320 \times 10^{-5} \text{ s m}^{-1}$  compared to the model estimated value of experimentally estimated values (Table 4). The remaining three burned plots had such high measured erosion values that WEPP underpredicted erosion even when using a very large  $K_r$  value ( $99.999 \times 10^{-3} \text{ s m}^{-1}$ ). On all eight non-burned plots (only 5 of which produced runoff) good agreement was achieved with optimized  $K_r$  values (Fig. 6). Optimized  $K_r$  values for the non-burned plots ranged from  $0.315 \times 10^{-3}$  to  $3.734 \times 10^{-3} \text{ s m}^{-1}$  compared with experimentally estimated and WEPP estimated values (Table 4).

These data suggest that the effect of fire on rill erodibility (4400% increase) is greater than was measured (800% increase) in the rill experiments. This may be related to the fact that rill experiments were conducted after a significant, erosion event (high intensity rainfall simulation). The rill experiments indicated that even during a 12-min period rill erodibility decreases significantly.

Prescribed fire increased mean  $K_r$  values by nearly two orders of magnitude (Table 4). It seems reasonable that loss of surface soil organic matter by fire (Soto and Diaz-Fierros, 1998) could result in increased rill erodibility. Fire consumes organic matter that binds soil particles together making them more difficult to detach (Pierson et al., 2001). Currently WEPP has no mechanism to incorporate this effect. WEPP users would have to estimate the effect of fire on  $K_r$  and  $\tau_c$  and modify their soil file to incorporate the effect of fire. There may be justification for introducing a burning adjustment to  $K_r$  for rangelands in WEPP. This would be similar to the adjustment made to  $K_r$  due to additions of residue, live roots, dead roots, and sealing and crusting effects for cropland.

## 5. Summary

Runoff and erosion from rainfall simulation experiments on steep sagebrush rangeland greatly increased immediately after prescribed burning. Runoff was generated more rapidly and volume was greater from burned plots compared to non-burned

plots. Soil erosion increased 100 times following the prescribed fire. The results from this study and other studies show that rill erosion is the dominant erosion process following fire. In order to provide adequate erosion predictions following fire, modeling efforts must emphasize the rill erosion process.

The ability of the WEPP model to predict fire impacts on soil erosion was tested using field data. The WEPP model allows users to specify rangeland burning through a reduction in the above ground biomass which influences hydraulic roughness and soil shear, but not soil rill erodibility. Using standard WEPP rangeland parameterization routines, WEPP underestimated soil erosion for burned conditions by an order of magnitude.

Rill experiments revealed relatively large discrepancies in rill width–discharge relationships between WEPP and measured data. Darcy–Weisbach roughness coefficients were more different between treatments than WEPP predicted. Measured rill erodibility was greater than WEPP estimated for the burned treatment. Rill erodibility was dynamic, decreasing with time.

WEPP erosion predictions were improved for the burned condition by replacing WEPP estimated parameters with measured parameters from the rill experiments, but agreement with measured erosion values was not achieved on all plots. To get good agreement with measured erosion required optimization of  $K_r$  values in the burned plots. The optimized values were significantly greater than those measured in the rill experiments. This is likely due to a decrease in  $K_r$  values from the beginning of the rainfall simulation through the end of the rill experiments. Adjustments to  $K_r$  are needed to account for increases in erodibility following burning. In addition, rill width and Darcy–Weisbach roughness coefficient parameters need to be better estimated. These parameters are important for predicting the flow erosivity and the amount of rill area subject to rill detachment and available for sediment transport.

## References

- Alberts, E.E., Moldenhauer, W.C., Foster, G.R., 1980. Soil aggregates and primary particles transported in rill and interrill flow. *Soil Science Society of America Journal* 44, 590–595.
- Calder, I.R., 1986. The influence of land use on water yield in upland areas of the U.K. *Journal of Hydrology* 88, 201–211.
- Cleveland, W.S., 1979. Robust locally weighted regression and smoothing scatterplots. *Journal of the American Statistical Association* 74, 829–836.
- Elliot, W.J., Liebenow, A.M., Laflen, J.M., Kohl, K.D., 1989. A compendium of soil erodibility data from WEPP cropland soil field erodibility experiments 1987 & 88, NSERL Report No. 3. US Department of Agriculture, Agricultural Research Service, National Soil Erosion Research Laboratory, West Lafayette, IN.
- Elliot, W.J., Robichaud, P.R., Hall, D.E., Cuhaciyani, C.O., Pierson, F.B., Wohlgemuth, P., 2001. A probabilistic approach to modeling erosion for spatially-varied conditions. American Society of Agricultural Engineers Annual Meeting, Sacramento, CA. July 2001. Paper No. 01-8006. 16 pp.
- Flanagan, D.C., Ascough II, J.C., Nicks, A.D., Nearing, M.A., Laflen, J.M., 1995. Overview of the WEPP erosion prediction model, p. 1.1–1.12. In: Flanagan, D.C., Nearing, M.A. (Eds.), *USDA-water erosion prediction project hillslope profile and watershed model documentation*, NSERL Report No. 10. US Department of Agriculture, Agricultural Research Service, National Soil Erosion Research Laboratory, West Lafayette, IN.
- Foster, G.R., 1982. Modeling the erosion process. *ASAE Monograph*, vol. 5. ASAE, Saint Joseph, Michigan, pp. 297–380.

- Foster, G.R., Flanagan, D.C., Nearing, M.A., Lane, L.J., Risse, L.M., Finkner, S.C., 1995. Hillslope erosion component, p. 11.1–11.12. In: Flanagan, D.C., Nearing, M.A. (Eds.), USDA-water erosion prediction project hillslope profile and watershed model documentation, NSERL Report No. 10. US Department of Agriculture, Agricultural Research Service, National Soil Erosion Research Laboratory, West Lafayette, IN.
- Gilley, J.E., Kottwitz, E.R., Simanton, J.R., 1990. Hydraulic characteristics of rills. *Transactions of the ASAE* 33, 1900–1906.
- Harkness, A.L., 1998. Soil Survey of Owyhee County Area, Idaho. USDA–NRCS. U.S. Gov. Printing Office, Washington, D.C.
- Hester, J.W., Thurow, T.L., Taylor, J.C.A., 1997. Hydrologic characteristics of vegetation types as affected by prescribed burning. *Journal of Range Management* 50, 199–204.
- Holland, M.E., 1969. Colorado State University experimental rainfall–runoff facility, design and testing of rainfall system. Tech. Rep. Colorado State University Experiment Station. CER 69-70 MEH 21.
- Johansen, M.P., Hakonson, T.E., Breshears, D.D., 2001. Post-fire runoff and erosion from rainfall simulation: contrasting forests with shrublands and grasslands. *Hydrological Processes* 15, 2953–2965 (URL <http://dx.doi.org/10.1002/hyp.384>).
- Moffet, C.A., Zartman, R.E., Wester, D.B., Sosebee, R.E., 2005. Surface bio-solids application: effects on infiltration, erosion, and soil organic carbon in Chihuahuan Desert grasslands and shrublands. *Journal of Environmental Quality* 34 (1), 299–311 (URL <http://jeq.scijournals.org/cgi/content/abstract/34/1/299>).
- Nearing, M.A., Foster, G.R., Lane, L.J., Finkner, S.C., 1989. A process-based soil erosion model for USDA-Water Erosion Prediction Project technology. *Transactions of the ASAE* 32, 1587–1593.
- Neter, J., Kutner, M.H., Nachtsheim, C.J., Wasserman, W., 1996. *Applied Linear Regression Models*, 3rd Edition. Irwin, Chicago, IL.
- O’Dea, M.E., Guertin, D.P., 2003. Prescribed fire effects on erosion parameters in and perennial grassland. *Journal of Range Management* 56, 27–32.
- Pierson, F.B., Robichaud, P.R., Spaeth, K.E., 2001. Spatial and temporal effects of wildfire on the hydrology of a steep rangeland watershed. *Hydrological Processes* 15, 2905–2916.
- Pierson, F.B., Carlson, D.H., Spaeth, K.E., 2002a. Impacts of wildfire on soil hydrological properties of steep sagebrush–steppe rangeland. *International Journal of Wildland Fire* 11, 145–151.
- Pierson, F.B., Spaeth, K.E., Weltz, M.A., Carlson, D.H., 2002b. Hydrologic response of diverse western rangelands. *Journal of Range Management* 55, 558–570.
- Pierson, F.B., Robichaud, P.R., Spaeth, K.E., Moffet, C.A., 2003. Impacts of fire on hydrology and erosion in steep mountain big sagebrush communities. In: Renard, K.G., McElroy, S.A., Gburek, W.J., Canfield, H.E., Scott, R.L. (Eds.), *First Interagency Conference on Research in the Watershed*, October 27–30, 2003. U.S. Department of Agriculture, Agricultural Research Service, pp. 625–630.
- Robichaud, P., Elliot, W.J., Hall, D.E., Pierson, F.B., Moffet, C.A., 2005. Erosion risk management tool (ERMiT). U.S. Department of Agriculture, Forest Service, Rocky Mountain Research Station, Moscow, ID. URL <http://forest.moscowfs.fsl.wsu.edu/cgi-bin/fswepp/ermit/ermit.pl>.
- Soto, B., Diaz-Fierros, F., 1997. Soil water balance as affected by throughfall in gorse (*Ulex europaeus*, L.) shrubland after burning. *Journal of Hydrology* 195, 218–231.
- Soto, B., Diaz-Fierros, F., 1998. Runoff and soil erosion from areas of burnt scrub: comparison of experimental results with those predicted by the WEPP model. *Catena* 31, 257–270.
- Yalin, M.S., 1963. An expression for bed-load transportation. *Proceedings of the American Society of Civil Engineers, Journal of the Hydraulics Division* 89 (HY3), 221–250.